MAGNETOHYDRODYNAMICS Vol. 61 (2025), No. 1–2, pp. 129–137
DOI: 10.22364/mhd.61.1–2.13

STABILITY OF TWO FLOWING COAXIAL FERROFLUID ANNULI

S.H. Ferguson Briggs[1], *M.G. Blyth*[2], *A.J. Mestel*[1]

[1] *Mathematics Department, Imperial College London SW7 2BZ, UK*
[2] *University of East Anglia, Norwich, NR4 7TJ, UK*

Two concentric ferrofluid annuli fill the gap between two concentric cylinders. In a stationary state without magnetic field, the interface between the fluids is unstable to surface tension. However, this instability can be controlled either by axial motion if the fluids have different viscosity, or by passing a current down the inner cylinder if the inner fluid has a higher magnetic susceptibility. If the susceptibilities differ, an axial magnetic field may also grant stability to all but the longest wavelengths. Each of these mechanisms can, however, give rise to other instabilities. This paper investigates the linear stability to arbitrary disturbances of the combination of shear and magnetic effects.

Introduction.

Ferrofluids react instantaneously to magnetic fields and so provide a mechanism for flow control. There is a growing number of applications in a variety of geometries [3, 5, 12, 14]. In this paper we consider an axisymmetric thread injection process with medical and industrial coating applications. A central wire is surrounded by a fluid annulus which is itself surrounded by a second fluid annulus and a solid outer boundary. The fluids have different physical properties. Depending on the application, the inner fluid may be more or less viscous than the outer, and be more or less magnetically susceptible.

The two fluids are labelled 1 and 2 and we use those suffices to denote quantities in the two fluids. They are assumed to have the same density ρ, but in general different viscosities μ_1, μ_2 and magnetic susceptibilities χ_1, χ_2. We nondimensionalise distances with respect to the interface radius, so that in terms of the cylindrical polar coordinates (r, θ, z), a solid wire occupies $0 < r < R_0$. Fluids 1 and 2 occupy $R_0 < r < 1$ and $1 < r < R_2$, respectively, while $r = R_2$ is a stationary, solid boundary as in Fig. 1. An axial pressure gradient F acts, giving rise to a unidirectional flow of the form $(0, 0, W_i)$

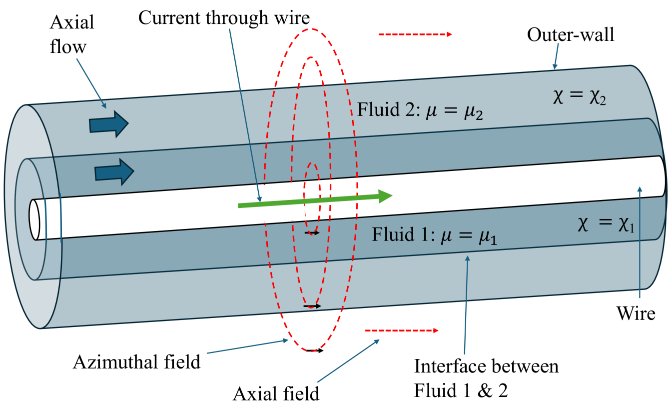

Fig. 1. Schematic of the two-fluid problem. The initial challenge is to control the interfacial instability at $r = 1$.

for $i=1,2$, where

$$W_1 = A_1 + B_1 \log r - \frac{\mathrm{Fr}^2}{4\mu_1}, \qquad W_2 = A_2 + B_2 \log r - \frac{\mathrm{Fr}^2}{4\mu_2}. \tag{1}$$

The wire is stationary in some applications, but we permit it to translate with a velocity (0, 0, V). The constants A_i and B_i, which are given explicitly in [6], follow from no-slip on $r=R_0$, R_2 and continuity of the velocity and tangential stress at $r=1$. As $(\mu_i \mathrm{d}W_i/\mathrm{d}r)$ is continuous at $r=1$, a jump in viscosity leads to a jump in dW/dr at the fluid interface, which is able to control the Rayleigh–Plateau instability [10, 13] if the flow is large enough [4, 11]. This is especially the case when the inner fluid is the more viscous. However, the resulting flow profile may be prone to hydrodynamic instabilities, especially at a high Reynolds number.

The capillary instability may also be controlled using magnetic fields. As the magnetic susceptibility is piecewise constant, magnetic effects are only felt at the interface and give rise to a jump in normal stress. Provided the inner ferrofluid is more magnetic than the outer, a sufficiently strong axial current $(0,0,J_0)$ can stabilise a stationary configuration. Note that in this case the normal stress has the opposite sign compared to the familiar pinch effect surrounding a current in MHD. A uniform axial field $(0,0,H_0)$ can also restrict the instability to long wavelengths, with or without the current [7].

1. Formulation of the problem.

We assume the ferrofluids are Newtonian with velocity $\mathbf{u}$ and pressure p. We assume a linear magnetisation law, so that the magnetic field and intensity are related by $\mathbf{B}=\mu_0(1+\chi)\mathbf{H}$, where μ_0 is the vacuum permeability. The governing equations then take the form

$$\nabla \cdot [(1+\chi)\mathbf{H}] = 0, \qquad \nabla \times \mathbf{H} = 0. \tag{2}$$

We assume χ is constant within each fluid, so that $\nabla^2\Phi=0$, where $\mathbf{H}=\nabla\Phi$. At the boundaries, normal $\mathbf{B}$ and tangential $\mathbf{H}$ are continuous. In the wire it is assumed that $\chi=0$. At the fluid interface there is a jump of magnetic stress, but no magnetic body force acts in the interior of each fluid, so that the velocity satisfies

$$\rho \frac{\mathrm{D}\mathbf{u}}{\mathrm{D}t} = -\nabla p + \mu_i \nabla^2 \mathbf{u}, \qquad \nabla \cdot \mathbf{u} = 0, \tag{3}$$

where $\mathrm{D}/\mathrm{D}t$ is the material derivative. The fluid equations hold separately in each fluid with the appropriate viscosity, μ_1 or μ_2. Continuity of the velocity is imposed at the boundaries $r=R_0$, 1, R_2. At the fluid interface the tangential component of the total stress (hydrodynamic and magnetic) is continuous, while the normal component jumps by an amount $\sigma\nabla\cdot\hat{\mathbf{n}}$, where σ is the surface tension and $\hat{\mathbf{n}}$ is the unit normal.

The equilibrium is perturbed so that the interface $r=1$ becomes

$$r = 1 + \varepsilon\zeta \qquad \text{where} \qquad \zeta = \mathrm{e}^{\mathrm{i}kz + \mathrm{i}m\theta + st}, \tag{4}$$

where the real part is implicitly assumed. Here ε is small and positive, the growth rate s may be complex, but the wavenumbers k and m are real. We take $k \geq 0$, while m is an integer but may be of either sign or zero. In each region the velocity, pressure and magnetic field are correspondingly perturbed in the form

$$\mathbf{u} = (0,\, 0,\, W_i(r)) + \varepsilon\zeta\mathbf{u}_i'(r), \qquad p = p_0 + \varepsilon\zeta p_i'(r), \tag{5}$$

and

$$\mathbf{H} = \left(0,\, \frac{J_0}{2\pi r},\, H_0\right) + \varepsilon\nabla(\zeta\phi_i(r)), \tag{6}$$

and the system is linearised. Here p_0 includes the pressure gradient $-Fz$ and the leading order discontinuity due to surface tension.

In the absence of a base flow, so that $F=0$ and $V=0$, the problem can be solved exactly in terms of modified Bessel functions. It was shown in [7] that the stability is then governed by the sign of the jump in normal stress across the perturbed surface, which takes the form

$$T_n = \sigma(1-k^2-m^2) - C_1(\chi_1-\chi_2)J_0^2 - C_2\left(kH_0 + \frac{mJ_0}{2\pi}\right)^2(\chi_1-\chi_2)^2. \tag{7}$$

Here C_1 and C_2 are known positive functions of k, m, R_0, R_2 and χ_2/χ_1. A given mode is found to be stable if $T_n<0$ and unstable if $T_n>0$.

Expression (7) is very instructive. The first term is the capillary term, which is destabilising for $0<k<1$ and $m=0$ [10, 13]. This can be controlled by a sufficiently large axial current J_0, provided the inner fluid is more magnetic than the outer, $\chi_1>\chi_2$. If the converse holds, the axial current is destabilising, in a manner akin to magnetic pinching in regular MHD. The final term in Eq. (7) is non-negative and hence always stabilising when the susceptibilities differ. If $m\geq 0$ and $k\neq 0$, then a sufficiently large axial field H_0 can guarantee stability [7]. However, if $m<0$, then for a suitable value of k the third term vanishes. The magnetic field lines on $r=1$ are helical and modes with $(0,\, m,\, k)$ everywhere normal to the local field are unaffected by this term. These modes are akin to the 'tearing modes' which cause trouble in Tokamak design [9]. If $m=0$, then for long enough waves ($k\to 0$) the capillary term dominates, since $C_1\to 0$. In practice there will be some limit on the possible axial wavelength.

Once the fluids are in motion, the stability behaviour is more complicated. The velocity field cannot be found in closed form and numerical techniques are required. We use a pseudospectral collocation approach, expanding the radial variation as series of Chebyshev polynomials. The expansions are truncated after typically 100 terms, reducing the system to a generalised eigenvalue problem of the form $A\mathbf{x}=sM\mathbf{x}$, where $\mathbf{x}$ is a vector of coefficients, while A and M are square matrices. The resultant system is solved in MATLAB. The code is verified by comparison with the results of [1, 4, 11], with closed form solutions at zero Reynolds number, and with long wave analysis as $k\to 0$.

We nondimensionalise velocities with respect to the capillary velocity scale σ/μ_1. In addition to the wavenumbers k and m, the full problem depends on ten parameters. We have the two geometric parameters, R_0 and R_2, the susceptibility χ_1, the ratios

$$\mu = \frac{\mu_2}{\mu_1} \qquad \text{and} \qquad \chi = \frac{\chi_2}{\chi_1}, \tag{8}$$

and three Reynolds numbers based on surface tension, the pressure gradient and axial wire velocity,

$$J = \frac{\rho R_1\sigma}{\mu_1^2}, \qquad G = \frac{\rho F R_1^3}{\mu_1^2}, \qquad W = \frac{\rho V R_1}{\mu_1}, \tag{9}$$

where we have reintroduced $R_1\equiv 1$ for dimensional clarity. There are also two magnetic parameters,

$$B = \frac{\mu_0 J_0^2}{4\pi^2 R_1\sigma}, \qquad Z = \frac{H_0}{J_0/(2\pi R_1)}. \tag{10}$$

The value $B=1$ is the current strength necessary to stabilise a stationary fluid cylinder. If $J_0=0$, we define B instead using H_0, formally using BZ^2 as the control parameter in place of B.

It is difficult to span such a large parameter space. Although general tendencies can be identified, exceptions can often be found as R_0 and R_2 vary. We begin by surveying the purely hydrodynamic case, which is analysed in detail in [6].

2. No magnetic effects.

Even the purely hydrodynamic stability is quite complicated, as discussed in [6]. We summarise here the important results. We will only consider here a stationary wire, $W=0$.

Firstly, when the fluid viscosities differ, the tangential stress continuity $\mu\,\mathrm{d}w/\mathrm{d}r$ requires a jump in $\mathrm{d}w/\mathrm{d}r$ at $r=1$. This discontinuous shear is able to mitigate the capillary instability. Fig. 2 shows contours of the real growth rate $\Re\{s\}$ as G and k vary, for $\mu=0.5$, $R_0=0.1$ and $R_2=1.3$. In Fig. 2*a* $J=1$, whereas Fig. 2*b* enlarges the small G region and also shows $J=100$. Fig. 2c enlarges a different region, not shown in Fig. 2*a*. For small G, the axisymmetric capillary instability can be seen, but this disappears at some value $G=G_L$. We call $G<G_L$ region 1. A separate instability (region 2) is found for $G>G_R$, which can involve various values of m. Flows with $G_L<G<G_R$ are stable. For this case, $G_L\simeq 10$ and $G_R\simeq 130$.

Increasing the surface tension parameter J increases the flow velocity G_L needed to stabilise region 1, as seen from Fig. 2b. Increasing J also increases G_R, banishing region 2 to high Reynolds number. The shape of region 1 suggests the value of G_L is attained as $k\to 0$. Analysis in this limit, following [4], shows

$$\Re\{s\} = k^2\left[\alpha(1-B) - \frac{1}{J}\left(\beta G^2 + \gamma W^2 + \delta W G\right)\right] + O(k^4), \tag{11}$$

where α, β, γ, δ are known in terms of R_0, R_2, χ_1, χ_2 and μ. For $W=0$, this predicts the value $G_L^2=\alpha J(1-B)/\beta$ which is in perfect agreement with Fig. 2*b*.

At large G, the flow may be prone to inviscid instabilities, as described by an axisymmetric equivalent of Rayleigh's inflection point theorem [2]. In [6], the criteria for this to occur are given, showing the flow in Fig. 2 is inviscidly stable. However, for these parameters, a third viscous instability appears, region 3 in Fig. 2c. The shape of this region alters very little as J varies and so the instability is impervious to surface tension. The reason for this can be deduced from Fig. 3, which depicts the unstable eigenfunctions in regions 1, 2, 3. Both instabilities for $m=0$ in region 1 and $m=1$ in region 2 demonstrate activity for all r, especially near the interface $r=1$. However, the region 3 instability is localised at the inner boundary and in the relatively thin outer fluid layer. The interface $r=1$ is hardly perturbed, indicating that this instability is generated by shear in the fluid interior rather than at the interface.

Region 3 instabilities exist only for some parameter regimes. For example, increasing $R_2=1.3$ to $R_2=2$ eliminates region 3, while regions 1 and 2 behave as before. In that case, complete stabilisation can be achieved for large enough G and J. Equally, there are cases, where regions 1 and 2 overlap and there is no stable interval $[G_L, G_R]$. Further, should the flow be inviscidly unstable, then it may be unstable for all G.

3. Magnetic effects.

Although there is some surprising behaviour, to a large extent, the effect of adding an axial field or current is similar to the above discussion of Eq. (7) for stationary fluid.

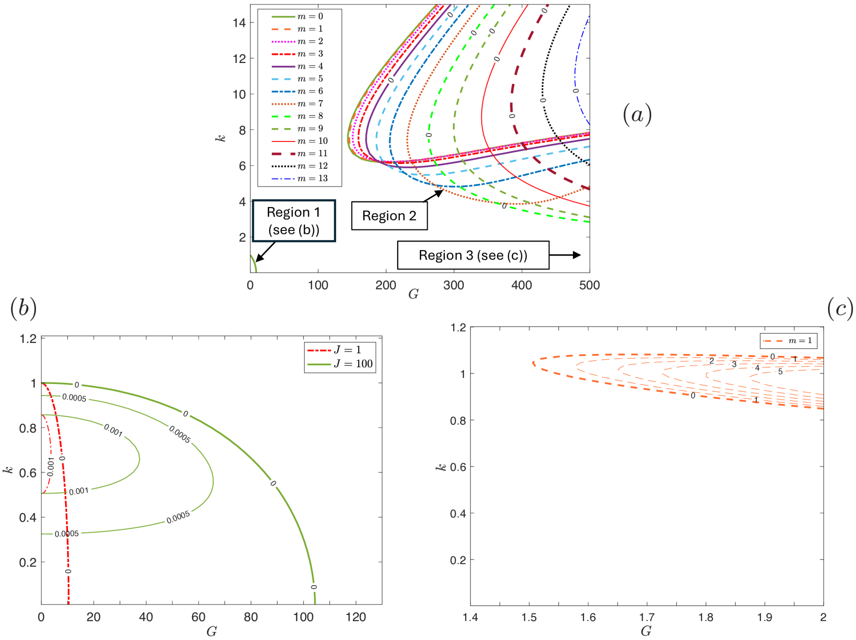

Fig. 2. Contours of $\Re\mathrm{e}\{s\}$ in the $(G,\, k)$ plane with no magnetic field for $R_0 = 0.1$, $R_2 = 1.3$ and $\mu = 0.5$. (a) $J = 1$: there are three instability regions. (b) Enlargement of region 1 for $J = 1, 100$. (c) Enlargement of region 3.

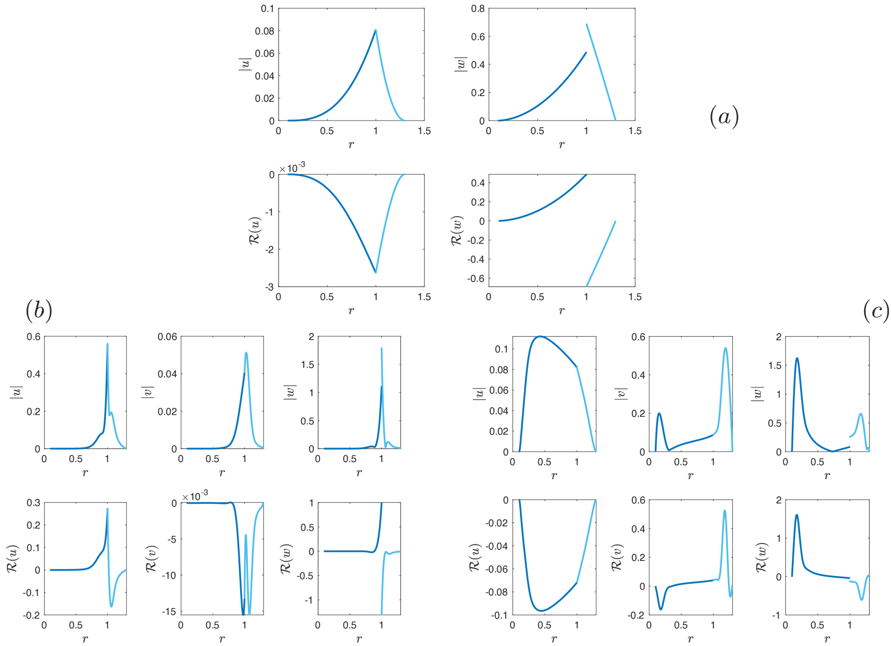

Fig. 3. Eigenfunctions for regions 1, 2, 3 for the parameters of Fig. 2. Left to right: u, v, w ($v = 0$ for $m = 0$.) w is discontinuous at $r = 1$. Top: absolute value, bottom: real part. (a) Region 1, $m = 0$, $k = 0.7$, $G = 5$, $s = 0.0075 - 0.7226\mathrm{i}$. ($b$) Region 2, $m = 1$, $k = 15$, $G = 1250$, $s = 8.903 - 4336\mathrm{i}$. ($c$) Region 3, $m = 1$, $k = 1$, $G = 20000$, $s = 5.911 - 1029\mathrm{i}$. Cases ($a$) and ($b$) are centred at the interface $r = 1$, but case (c) is not.

Thus, an axial current on the whole is stabilising if and only if the inner fluid is more susceptible ($\chi < 1$). Furthermore, the effect of an axial field is usually stabilising, except for the long waves as $k \to 0$, over which it has little influence. Simultaneously imposing both axial current and field gives rise to helical field lines. Even if the inner fluid is less magnetically susceptible, $\chi > 1$, strong enough fields tend to stabilise all modes save those for which $kZ + m \simeq 0$. Should such modes be hydrodynamically stable, then complete linear stabilty can be achieved.

By way of illustration, we take the case shown in Fig. 2 and add an axial current with the inner fluid more magnetic, $\chi_1 = 5$, $\chi_2 = 0$. Fig. 4a shows the case for $B = 10$. As $B = 1$ is the threshhold for stabilising the capillary mode, there is no region 1. Region 2 is moved towards higher G but still exists. A number of m-modes are unstable and $m = 0$ is the first instability as G increases past G_L. Region 3 is hardly affected by the field.

In Fig. 4*b*, we instead add an axial field of comparable strength, $BZ^2 = 10$, this time with $\chi_1 = 0$, $\chi_2 = 5$. This stabilises region 1 when $k = O(1)$, but the long waves ($k \to 0$) are not controlled, as indicated in the inset. Physically, the field lines are only slightly distorted by long axisymmetric waves, and the instability persists, albeit with a slower growth rate. Region 2 is again moved to higher G, but the lower m-modes

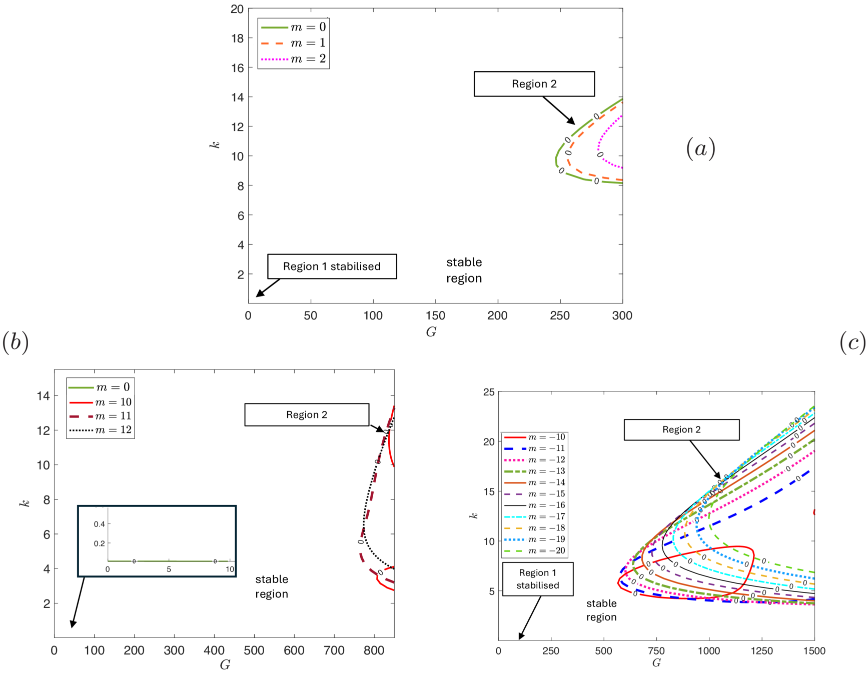

Fig. 4. Stability for the parameters of Fig. 2 with a magnetic field. (*a*) Axial current $B = 10$, $\chi_1 = 5$, $\chi_2 = 0$. Region 1 is stabilised, region 2 is shifted to higher G. Several m are unstable, but $m = 0$ the most. (*b*) Axial field $BZ^2 = 10$, $\chi_1 = 0$, $\chi_2 = 5$: compared to Fig. 2, region 1 remains but is compressed down towards $k = 0$. The various m-modes comprising region 2 are all shifted towards larger G, but it turns out that $m = 11$ is now the first to go unstable. (*c*) Both axial and azimuthal fields, $\chi_1 = 5$, $\chi_2 = 0$, $B = 10$, $Z = 2$. Region 1 has been eliminated. Region 2 modes with $m \geq 0$ are now stable, but instabilities occur if $m + kZ$ is small. In each of (*a*), (*b*) and (*c*), region 3 exists at higher G and is almost unaffected by the field.

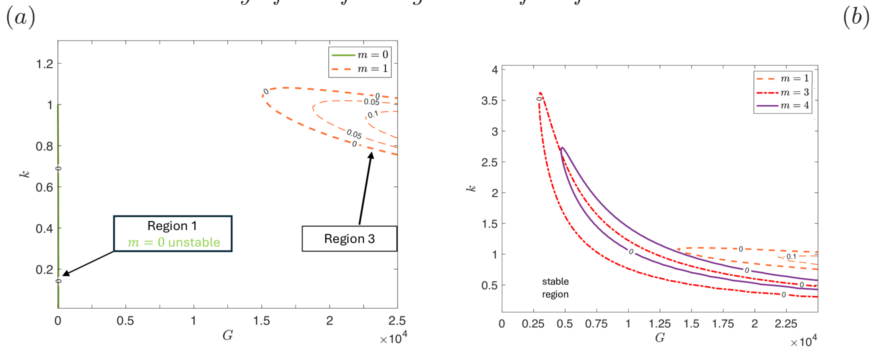

Fig. 5. Addition of azimuthal field may destabilise $m > 1$ for $R_0 = 0.1$, $R_2 = 2$, $\mu = 0.5$, $J = 100$, $\chi_1 = 5$, $\chi_2 = 0$. (*a*) $B = 0$, (*b*) $B = 100$.

require a higher G for instability and it transpires that $m = 11$ is the first to go unstable as G increases past G_L. Yet once more, we find that the unstable region 3 remains for almost identical G values. The growth rate increases slightly as BZ^2 increases. Finally, in Fig. 4c we include both axial and azimuthal fields. Whereas previously the sign of m was irrelevant, it is now critical. For these values, we find unstable modes if $kZ + m \simeq 0$. This effect may be still more pronounced at higher Z.

We see, therefore, that the instability regions 1 and 2 can in many parameter ranges be eliminated by combined axial and azimuthal fields. This is easier to accomplish when the inner fluid is more magnetically susceptible, but even when the converse holds, a strong enough axial field controls all but the spiral modes, for which $kZ + m \simeq 0$. Should such modes be hydrodyamically stable, then complete stability may be attained. However, the region 3 modes of Fig. 2 can prove impervious to magnetic effects, for the same reason that strong surface tension also had no effect. Both capillary and magnetic effects take place at the fluid interface, and the region 3 modes are concentrated near the boundaries with little disturbance of the interface $r = 1$. A very high value of JB (or JBZ^2) is needed to influence the region 3 modes at all and seems to destabilise them further. These modes are akin to those found by Heaton [8] and only exist for some geometries and parameter ranges. When they do occur, they require a moderately high Reynolds number and may not be of concern for some practical devices.

It is possible for the magnetic field to introduce unexpected new instabilities. For example, in Fig. 5, $R_0 = 0.1$, $R_2 = 2$, $\mu = 0.5$, $J = 100$, $\chi_1 = 5$ and $\chi_2 = 0$. When $B = 0$, panel 5a shows the familiar regions 1 and 3, as region 2 has been banished by the high surface tension. When $B = 100$ in Fig. 5b, region 1 disappears, but the $m = 1$ unstable modes of region 3 extend to lower G, as JB is now large enough to influence the viscous instability. More signficantly, $m = 3$, 4 are destabilised for much lower flow rates G. For these values $m = 2$ and $m \geq 5$ remain stable, but that is not the case for other values and still more complex behaviour is possible. This sensitivity to modes with $m > 1$ lessens as the wire thickness R_0 increases.

4. Concluding remarks.

We have shown that the stability of the two-ferrofluid annular flow is quite complicated, depending subtly on the particular geometry and fluid properties. For stationary fluid, stability requires an axial current and for the inner fluid to be the magnetically more susceptible. However, once the fluids are in motion, it is possible for the configuration to be stable without any field, exploiting the differential shear for different fluid viscosities. If that is not the case, a judicious combination of axial and azimuthal fields may regularise the system. Particular attention must in that case be paid to specific helical modes, which need to be controlled hydrodynamically. Non-axisymmetric modes are frequently the least stable and can be excited either hydrodynamically or magnetically. Investigation is continuing in order to understand the full problem in greater detail.

It is dangerous to oversimplify the flow behaviour, but in general terms, overall stability is more likely if the inner fluid is more viscous, if the inner fluid is more magnetic, if the pressure gradient is large enough but not too large, if an axial field is included and if the inner fluid thickness is less than that of the outer.

It should be remembered that the stability analysis of this paper is entirely linear. At high Reynolds numbers it is well known that subcritical bifurcations can occur which could lead to effective instability for non-infinitesimal disturbances at lower values of G. For a particular parameter set the linear results could be supplemented by DNS calculations. However, these would need to be fully three-dimensional, nonlinear and time-dependent and laborious to perform for the wide parameter space.

References

[1] M.G. Blyth, and A.P. Bassom. Stability of surfactant-laden core-annular flow and rod-annular flow to non-axisymmetric modes. *J. Fluid Mech.*, vol. 716 (2013), R13, pp. 1–13.

[2] S. Chandrasekhar. *Hydrodynamic and Hydromagnetic Stability.* OUP 1961.

[3] S.W. Charles. Some applications of magnetic fluids – use as an ink and in microwave systems. *J. Magn. Magn. Mater.*, vol. 65 (1987), pp. 350–358.

[4] H.A. Dijkstra. The coupling of interfacial instabilities and the stabilization of two-layer annular flows. *Phys. Fluids*, vol. 4 (1992),no. 9, pp. 1915–1928.

[5] A. Fattah, A. Rahman, S. Ghosh and I.K. Puri. Printing microstructures in a polymer matrix using a ferrofluid droplet. *J. Magn. Magn. Mater.*, vol. 401 (2016), pp. 1054–1059.

[6] S.H. Ferguson Briggs, M.G. Blyth, and A.J. Mestel. The stability of a two-fluid rod annular flow. *Phys. Rev. Fluids*, vol. 10 (2025), no. 3, 10.034001.

[7] S.H. Ferguson Briggs, A.J. Mestel. Linear stability of a ferrofluid centred around a current-carrying wire. *J. Fluid Mech.*, vol. 942 (2022), A20.

[8] C.J. Heaton. Linear instability of annular Poiseuille flow. *J. Fluid Mech.*, vol. 10 (2008), pp. 391–406.

[9] S.G. Mirnov, and I.G. Semenov. Investigation of the instabilities of the plasma string in the Tokamak-3 system by means of a correlation method. *Sov. J. Atom. Energy*, vol. 30 (1971), pp. 22–29.

[10] J.A.F. Plateau. Statique experimentale et theorique des liquides soumis aux seules forces moleculaires. *Gauthier-Villars*, vol. 3 (1873). Trubner and Co.

[11] L. Preziosi, K. Chen, and D.D. Joseph. Lubricated pipelining: stability of core-annular flow. *J. Fluid Mech.*, vol. 201 (1989), pp. 323–356.

[12] L. Preziosi and F. Rosso. Interfacial stability in a two-layer shearing flow between sliding pipes. *Eur. J. Mech. B Fluids*, vol. 10 (1991), pp. 269–294.

[13] L. Rayleigh. On the instability of jets. In: *Proc. the London Mathematical Society*, vols. 1–10 (1878), pp. 4–13.

[14] A.G. Walton. The linear and nonlinear stability of thread-annular flow. *Phil. Trans. R. Soc. A*, vol. 363 (2005), pp. 1223–1233.

Received 02.23.2024